

Spin Freezing In The Cuprate S=1/2 Antiferromagnetic Chain Compound SrCuO₂.

I. A. Zaliznyak^{1,2,†}, C. Broholm^{1,2}, M.Kibune³, H.Takagi³

¹*Department of Physics and Astronomy, The Johns Hopkins University, Baltimore, Maryland 21218*

²*National Institute of Standards and Technology, Gaithersburg, Maryland 20899*

³*ISSP, University of Tokyo, Roppongi, Tokyo 106, Japan*

(March 23, 2019)

We report neutron scattering study of the copper-oxide chain compound SrCuO₂ with antiferromagnetic spin-1/2 chains stacked in two-leg “zig-zag” ladders and coupled by very weak interchain interactions. Neither gap in magnetic fluctuations spectrum nor any evidence to the effect of zigzag coupling on static properties is observed. Below $T_{c1} = 4.9(1)\text{K}$ weak peak of elastic magnetic scattering appear at slightly incommensurate position $\mathbf{Q}_m \approx (0.506, 0, 0.5)$. Peak has unusual temperature dependence with cusp at $T_{c2} \approx 1.5\text{K}$ reminiscent of the phase transition and bears extremely small magnetic moment $\langle \mu_{Cu} \rangle = 0.030(5)\mu_B$ even at $T \approx 0.35\text{K}$. Its measurable physical width in the $a - b$ plane reveals finite and strongly anisotropic interchain correlations, with $\xi_a \approx 60a$, and very short $\xi_b \approx 2.2(5)$. Also about a half of the total magnetic intensity is completely independent of the wavevector transfer along \mathbf{b}^* . Thus, instead of 3D long-range order theoretically expected due to non-zero interchain couplings J'_a, J'_b , *quantum spin freezing* into anisotropic glassy structure is observed in SrCuO₂. It consists of rather well-correlated incommensurate two-dimensional layers of almost perfectly ordered chains stacked with little regard for the inter-plane coherence.

PACS numbers: 75.10.Jm, 75.40.Gb, 75.50.Ee

Interest in magnetic properties of S=1/2 antiferromagnetic chain compounds with particular emphasis on the novel mechanisms of the spin gap formation and destruction of the magnetic order in the ground state (G. S.) has been significantly renewed with the advent of the high-temperature superconductors. Significant progress in synthesis of new metal oxide materials that came along provided experimentalists with an access to large variety of new realizations of such systems. They commonly feature Cu²⁺ chains built from generic CuO₄ square plaquets with copper at the center, linked in either edge-sharing (La₆Ca₈Cu₂₄O₄₁, Li₂CuO₂, CuGeO₃) or corner-sharing (SrCuO₂, Sr₂CuO₃, Sr₁₄Cu₂₄Q₄₁) configuration [1,2]. In the latter nearest-neighbor copper spins are coupled by extremely strong antiferromagnetic exchange interaction $J \sim 2000\text{K}$ passing through nearly 180° Cu-O-Cu bond, similar to the well known example of La₂CuO₄. In a homologous series of Sr-based compounds Sr_nCu_{n+1}O_{2n+1} a number of the corner-sharing chains is stacked in a corner-sharing geometry to form conventional (n+1)-leg ladder with strong interchain coupling $J' \approx J$ within each ladder [3]. Theoretically these are expected to have dimerized G. S. and gapful spectrum when number of legs is even, and be in a gapless spin-fluid phase when it is odd [4]. SrCuO₂ is a unique material which does not belong to the above ladder class, although chemically it is a realization of the general formula at $n \rightarrow \infty$ and is considered to be a parent compound for a series. Instead, it contains corner-sharing Cu-O chains stacked pairwise in the edge-sharing geometry to form a two-leg “zigzag ladder” with very weak and possibly ferromagnetic $|J'| \lesssim 0.1J$ “zigzag” coupling between them realized through $\approx 87.7^\circ$ Cu-O-

Cu bonds [4,5]. Spin Hamiltonian of each zigzag unit is that of S=1/2 antiferromagnetic Heisenberg chain with next-nearest neighbor interaction (1D ANNH model), with zigzag interchain exchange $J' \equiv J_1$ playing the role of the nearest-neighbors coupling and in-chain exchange $J \equiv J_2$ the next-nearest neighbor one. After Haldane realized [6] that starting with rather small critical $J_{2c} \sim J_1/6$, S=1/2 ANNH chain has dimerized gapful G. S., this fascinating problem attracted much theoretical attention [7–10]. More recent renormalization group studies [7,8] and numerical calculations [8–10] supported appearance of the gapful phase at $J_{2c} \gtrsim 0.24J_1$. In the case $J_2 \gg J_1$ of the ladder with two weakly coupled chains realized in SrCuO₂, the gap is expected to be exponentially small, $\Delta \sim J_2 \exp(-\alpha J_2/J_1)$. Quantitatively, however, no reliable prediction for Δ can be made at the time, since theoretical estimates of the parameter α range from $\alpha = 1/(6\pi) \approx 0.053$ obtained in the field theory [7] to $\alpha \approx 1.6$ extrapolated from the numerical results [8] in the region $J_2/J_1 \leq 2.5$. Interestingly, in the case of small ferromagnetic $J_1 < 0$ which was briefly considered in [7], field theory predicts the model to remain critical, *i.e.* gapless, as is the single S=1/2 spin chain [11]. Another consequence of the critical nature of the G. S. in the latter is instability of its algebraic disorder with respect to the interchain coupling J' . If the correlation length ξ in S=1/2 chain system does not become restricted by some peculiar spin-gap-generating interactions [4,12], at sufficiently low $T \sim J'\xi \sim \sqrt{JJ'}$ any finite J' will make the long-range 3D Néel order favorable. We show in the present study, however, that neither spin gap nor conventional long-range 3D order realizes in SrCuO₂. Instead, a novel transition into a glassy state with finite

and anisotropic static correlations occurs, which we call *quantum spin freezing*.

SrCuO₂ crystallizes in the orthorhombic structure [13], space group D_{4h}^{17} ($Cmcm$), with four formula units per unit cell and lattice parameters $a = 3.556(2)\text{\AA}$, $b = 16.27(4)\text{\AA}$, $c = 3.904(2)\text{\AA}$. Its structure and bulk magnetic properties were studied by a number of authors [3,5,13–16]. In SrCuO₂ zigzag “ladders”, each formed by two chains running in c direction in b – c plane are stacked on a centered rectangular lattice in a – b plane. In this structure nuclear Bragg reflections (h, k, l) are only allowed for even $h+k$ and even l at $k = 0$, so that magnetic scattering at $\mathbf{Q} = (1/2+h, 0, 1/2+l)$ around the 1D antiferromagnetic zone center of the chains is not expected to produce any intensity at $\mathbf{Q}_\tau = (1/2-h, 0, 1/2-l)$. Dominant in-chain exchange $J_2 = 2100(200)\text{K}$ was determined [14] from temperature dependence of single crystal magnetic susceptibility. Interchain direct coupling in a direction J'_a is expected to be small, perhaps, accompanied by the next-nearest neighbor coupling J''_a of comparable magnitude passing through the oxygens. Exchange in b direction between the chains separated by more than 8\AA and large Sr ions is even more negligible. However small, these interactions are ultimately responsible for development of the interchain correlations in the G. S.

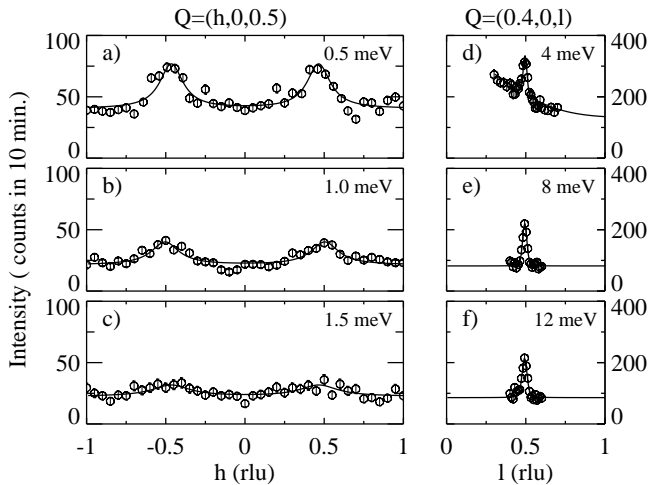


FIG. 1. Dependence of the inelastic magnetic scattering from SrCuO₂ on the wavevector transfer in \mathbf{a}^* direction perpendicular to the chains, (a)-(c), and along the chains (d)-(f). Sloping background in (d) comes from detector approaching the direct beam. Solid lines are fits described in text.

High-resolution neutron scattering experiments studying the spectral and spacial composition of spin correlations in SrCuO₂ were performed at NIST Center for Neutron Research using SPINS cold neutron and BT2, BT9 thermal beam 3-axis spectrometers in various configurations optimised for each particular measurement. PG(002) reflections were used for monochromator and analyser in all setups. The sample was a large $\approx 6 \times 6 \times 46\text{mm}$ rod-shaped crystal of SrCuO₂ of

$m = 3.875(5)\text{g}$; rod axis was at $\approx 15^\circ$ to $[001]$ direction. Its mosaic structure showed twinning with two roughly equal sharp peaks of $\text{FWHM} \approx 0.25^\circ$ separated by $\approx 0.5^\circ$ in the $(h, 0, l)$ plane, which was necessary to take into account for adequate description of elastic data. Except for the inelastic measurements shown in Fig. 1, (d)-(f) where the sample environment was displex refrigerator, sample was mounted in a pumped ³He cryostat which provided variable temperature down to $T \approx 0.35\text{K}$. Two sample orientations, with wavevector transfers in $(h, 0, l)$ and (h, k, h) reciprocal lattice planes, were studied.

Scans along the chain direction in the vicinity of the 1D antiferromagnetic point $l = 1/2$ in $(h, 0, l)$ plane were performed at constant energy transfers $E = 2 \div 14\text{meV}$ and $T = 12.5(5)\text{K}$ to check on the possible existence of the spin gap due to zigzag coupling J_1 , Fig. 1, (d)-(f). Thermal neutrons with fixed final energy $E_f = 14.7\text{meV}$ and collimations $60' - 60' - 80' - 120'$ for $E \geq 4\text{meV}$, and $E_f = 13.7\text{meV}$ and $60' - 40' - 40' - 120'$ for $E \leq 4\text{meV}$ were used. At all E sharp peak (resolution-convoluted fits to a Lorentzian shown in Fig. 1, (d)-(f) yield negligible physical width) centered at $l = 1/2$ is observed. It corresponds to scattering from spinon continuum in $S=1/2$ chain bounded by des Cloiseaux-Pearson relation $\epsilon(q) \geq \frac{\pi}{2}J \sin(qc)$, $q = \frac{2\pi l}{c}$. Due to very large value of $J = J_2 = 181(17)\text{meV}$, the width of the continuum in our range of energy transfers is smaller than (energy integrated) instrument resolution $R_l \gtrsim 0.035\text{rlu}$, and its structure with maxima at the boundaries is not resolved. Peak integral intensity remains roughly constant at all energies, as expected for the spinon continuum, providing evidence to the absence of the gap exceeding $\sim 0.2\text{meV}$ in the spin excitations spectrum of SrCuO₂. This result suggests very small and possibly – ferromagnetic interchain zigzag coupling $|J_1| \lesssim 0.1J_2$ in agreement with [4].

Dependence of the inelastic peak intensity at $l = 0.5$ on the wavevector transfer along \mathbf{a}^* was measured on SPINS at energy transfers in $0.5 \div 2\text{meV}$ range using neutrons with $E_f = 5.1\text{meV}$, collimations $80' - 80' - 240'$ and Be filter after the sample at $T = 0.35\text{K}$, Fig. 1 (a)-(c). Broad peaks centered at $|h| \approx 0.5$ and spanning the better part of the Brillouin zone are observed (note that wavevector scale in both panels of Fig. 1 is roughly the same highlighting the anisotropic peak width in two directions). Such “condensation” of the low-energy spin fluctuations to the vicinity of the wavevector $q = \pi/a$ along \mathbf{a}^* is a sign of weak antiferromagnetic interchain coupling. With increasing energy peaks broaden at a rate $(\pi v_a)^{-1} = 0.14(5)\text{rlu/meV}$, but their splitting into dispersive modes is not observed. From the broadening rate we can estimate $J'_a \sim v_a \approx 2.5\text{meV}$. At higher energies this antiferromagnetic modulation disappears and change of intensity with h within the experimental error could be attributed to Cu²⁺ magnetic formfactor.

In line with the above inelastic data, elastic scattering at $T = 0.35\text{K}$ is also peaked at $\mathbf{Q}_m \approx (0.5, 0, 0.5)$,

revealing some kind of static spin ordering in the system. Net elastic intensity shown in Fig. 2 was obtained by subtracting background data collected in same scans at $T=8K$ where magnetic scattering disappear. Scans in the (h, k, h) plane, Fig. 2(a), were performed using thermal neutrons with $E_f = 14.7$ meV and collimations $60' - 40' - 40' - 120'$, while $(h, 0, 0.5)$ and $(0.507, 0, l)$ scans shown in Fig. 2(b),(c) were collected on SPINS at $E_f = 3.7$ meV and collimations $80' - 40' - 240'$. In all elastic setups multiple filters were placed in the beam to suppress its contamination by neutrons from higher order reflections in monochromator to less than 1 count per minute.

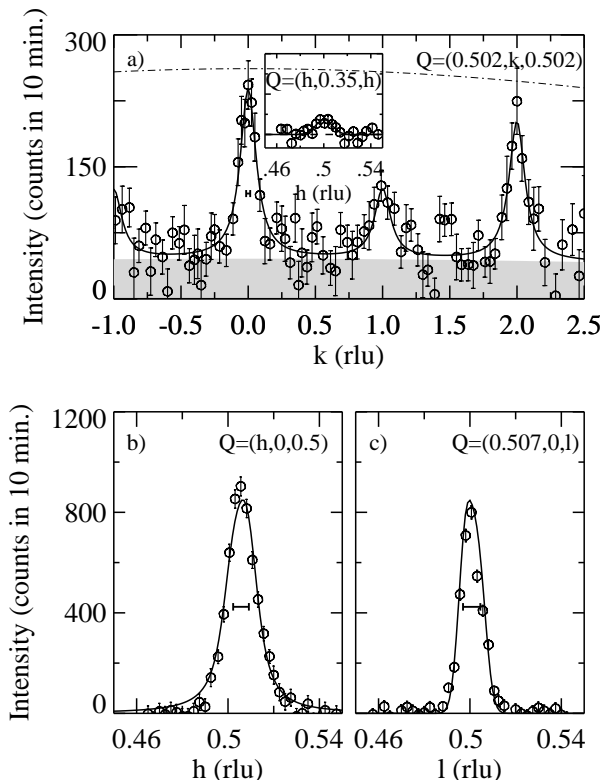


FIG. 2. (a)-(c) wavevector dependence of the net elastic intensity around $\mathbf{Q} \approx (0.5, 0, 0.5)$ at $T=0.35K$ along \mathbf{b}^* , \mathbf{a}^* and \mathbf{c}^* directions respectively. Horizontal bars show calculated FWHM of the instrument resolution function at the peak position. Solid lines are resolution convoluted fits described in text. In (a) shaded area shows k -independent “magnetic rod” intensity; dash-dotted curve on the top is variation of the Cu^{2+} magnetic formfactor within the scan range; insert shows scan across the rod away from the peak at $k = 0.35$.

There are two outstanding features in Fig. 2(a) which demonstrate right away that observed elastic peaks do not result from a usual 3D long-range magnetic order. First, there is a substantial physical width to the peaks in \mathbf{b}^* direction, much larger than the instrument resolution, which implies finite and rather short correlation length ξ_b . Solid line in Fig. 2(a) shows a fit of the exper-

imental points with a sum of equal-width Lorentzians at integer k , which yields $\xi_b = 2.2(5)b$. In addition, about half of the total elastic intensity appears as “2D rod” of magnetic scattering completely independent of k , shaded area in Fig. 2(a). Insert shows the $(h, 0.35, h)$ scan across this rod which, like the h -scan at the top of the peak at $k = 0$ is resolution limited. Both peaks at odd k , implying antiferromagnetic correlations between corner and body-center chains, and at even k pointing to their ferromagnetic alignment are observed. Thus, in the G. S. of SrCuO_2 zigzag chains are only partially correlated in \mathbf{b}^* direction, and this short-range structure is either double- Q or comes in short pieces correlated either way.

High-resolution scans in $(h, 0, l)$ plane, Fig. 2(b),(c), also revealed that peak has finite width in \mathbf{a}^* direction. For quantitative analysis of the data we approximate finite-width peak lineshape by factorized Lorentzians employing the following expression for the elastic structure factor around $k = 0$,

$$\begin{aligned} S_0^\alpha(\mathbf{q}) &= \langle S^\alpha \rangle^2 \frac{V^*}{\pi} \frac{\kappa_h}{\kappa_h^2 + (q_h - a^* h_0)^2} \\ &\times \left(\frac{I_r}{b^*} + \frac{1 - I_r}{\pi} \frac{\kappa_k}{\kappa_k^2 + q_k^2} \right) \delta(q_l - c^* l_0), \end{aligned} \quad (1)$$

where $\langle S^\alpha \rangle$ is $\alpha (= x, y, z)$ component of the local ordered spin $\langle S \rangle$ at each site, for the isotropic spin system without long-range order we expect $\langle S^\alpha \rangle = \frac{1}{3} \langle S \rangle$, V^* is the volume of the reciprocal lattice unit cell, $\kappa_j = 1/\xi_j$ are the inverse correlation lengths, and I_r is relative contribution of the k -independent “rod” intensity, which according to fit in Fig. 2(a) amounts to $I_r = 0.51(9)$. $S_0(\mathbf{q})$ is elastic part of the dynamic structure factor $S^\alpha(\mathbf{q}, E) = S_0^\alpha(\mathbf{q})\delta(E) + S_{inel}^\alpha(\mathbf{q}, E)$, which define the unpolarized neutrons differential scattering cross-section

$$\frac{d^2\sigma}{dE d\Omega} = N \frac{k_i}{k_f} \left(r_0 \frac{g}{2} F(q) \right)^2 \sum_\alpha \left(1 - \frac{q_\alpha^2}{q^2} \right) S^\alpha(\mathbf{q}, E), \quad (2)$$

where $r_0 = 5.38 \cdot 10^{-13}$ cm, N is number of Cu^{2+} ions, $g = 2.15$ is their g -factor [16], and $F(q)$ is Cu^{2+} magnetic formfactor. Solid curves in Fig. 2(b),(c) result from the resolution convoluted global fit of scans in both directions to the neutron scattering cross-section defined by (1),(2) for two equivalent mosaic blocks inclined at $\eta \approx 0.5^\circ$ to each other. Peak intensity, position h_0, l_0 in reciprocal space and width $2\kappa_h$ were varied.

Fits to data measured in various setups at $T \approx 0.35K$ all yield similar values for peak intensity and position, scattered only within the statistical error and wavevector accuracy $\delta q/q \sim 2 \cdot 10^{-3}$ defined by the instruments angular precision. If the misalignment of the mosaic blocks was allowed to vary it was consistently refined to $\eta \approx 0.5(1)^\circ$, in agreement with nuclear Bragg scattering. We find that peak is centered at $l_0 = 0.500(1)$ along the chain, so that incommensurability $l_0 = 0.5 + \delta l$

expected in ANNH model with classical spins is not observed. This implies either very small frustrating zigzag interaction, $|J_1/J_2| \approx 4\delta_l \lesssim 0.004$, or that classical prediction is not valid in quantum $S=1/2$ case. On the other hand, peak is slightly off the antiferromagnetic position along \mathbf{a}^* , at $h_0 = 0.506(1) = 0.5 + \delta_h$. This indicate incommensurate helical interchain correlations in a direction with pitch $\zeta \approx 167a$, which could be explained by competition of the antiferromagnetic direct exchange J'_a between the nearest neighbor chains and superexchange J''_a between the next-nearest neighbor chains.

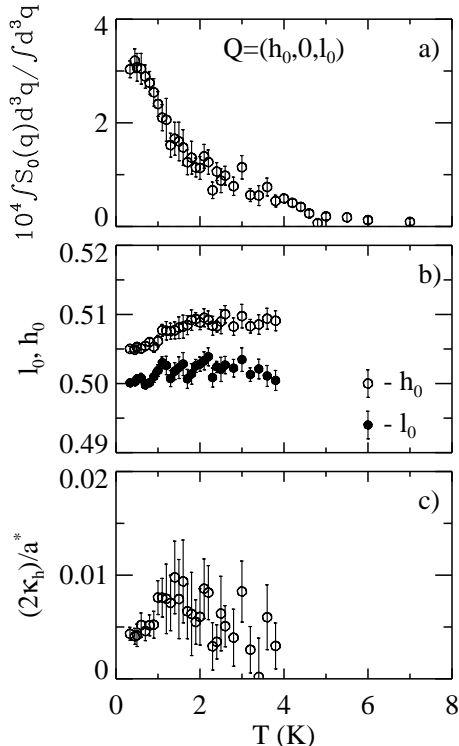


FIG. 3. Temperature dependencies of the peak parameters in the elastic structure factor (1) refined in the global resolution convoluted fit.

Peak width $2\kappa_h$, comparable to the mosaic splitting and instrument resolution, is quite sensitive to the deconvolution procedure. Its value refined in different experimental setups range from $2\kappa_h = 0.009(1)a^*$ for data shown in Fig. 2 to $2\kappa_h = 0.004(1)a^*$. This width, however, is always definitely non-zero, so that correlation length in \mathbf{a}^* direction is clearly finite, although we can only define it with rather large tolerance $\xi_a = 58(26)a$. Such anisotropic character of the interchain correlations imply $J'_a \gg J'_b$, consistent with SrCuO_2 crystal structure.

Using scattering from either the Vanadium standard or sample weaker nuclear Bragg reflections to calibrate the volume of the instrument resolution, we consistently find that refined peak intensity at $T = 0.35\text{K}$ correspond to very small ordered spin value $\langle S \rangle = 0.030(5)S$.

Temperature dependence of the peak parameters shown in Fig. 3 was measured in a number of scans similar to those in Fig. 2(b),(c) but with shorter counting time, using neutrons with $E_f = 4.47\text{meV}$ and collimations $80' - 80' - 240'$. Elastic intensity appears below $T_{c1} = 4.9(1)\text{K}$ and increase roughly linearly with $T_{c1} - T$ down to $T_{c2} = 1.5(3)\text{K}$, where it starts to increase at ~ 5 times faster rate to saturate below $T \sim 0.5\text{K}$. Neutron intensity was converted to the structure factor shown in Fig. 3(a) using V sample in similar geometry as a reference; error bars in the figure do not account for T-independent systematic error $\sim 20\%$ resulting from this procedure. While peak position along the chain l_0 remains within the experimental error temperature independent, its incommensurability δ_h in \mathbf{a}^* direction decrease below T_{c2} (between 2K and 1K) about twice, signaling the corresponding increase in the pitch of helical correlations, Fig. 3(b). Peak width $2\kappa_h$ is also found to be temperature dependent, Fig. 3(c), decreasing at low T (interchain correlations grow) after some hint of critical anomaly at T_{c2} .

Unusual temperature behaviour hints to the possible origin of the short-range static order in SrCuO_2 , peculiar to weakly coupled low-dimensional spin systems with ordered or critical ground state but with no order at $T > 0$, which we refer to as *quantum spin freezing*. At low T disorder restricting the correlation range in such systems can be described as a gas of thermally excited order-destroying topological defects: solitons in 1D or vortices in 2D. With decreasing temperature the equilibrium density of such defects goes down, and the correlation length ξ diverges at $T \rightarrow 0$. As was discussed for the case of $S=1/2$ chain, in such situation any finite coupling J' between the systems is expected to produce long-range order at finite $T_c \sim J'\xi$. It may happen, however, that this temperature T_c is lower than the characteristic pinning energy E_p of the above topological defects to the impurities or crystal lattice faults present in real materials. Then, at $T_{c1} \sim E_p > T_c$ order-destroying defects become *static*, with thermal energy being insufficient to move them, and the whole spin structure *freeze*. Below this temperature *local* ordered spins appear arranged in a *static* structure which looks like an instantaneous picture of the *dynamic* correlations just above freezing. In terms of the contribution to the structure factor, its dynamic range shrinks to zero with little change in the wavevector distribution of the energy-integrated intensity. Helical interchain correlations are naturally expected in such state, reflecting the structure of the frozen defects. In fact, their density (\equiv size) define both incommensurability δ_h and the correlation length ξ_a , in consistence with very close values $\delta_h \sim 2\kappa_h$ found experimentally. With increasing role of interplane correlations along \mathbf{b}^* at $T = T_c$ a decrease in the defects density can be expected, which also explain the anomaly at $T_{c2} = T_c$ with both δ_h and κ_h decreasing roughly twice.

We thank I. Affleck and G. Shirane for interest and helpful remarks, R. Erwin for help with experiments. This work was based upon activities supported by NSF under Contract No. DMR-9423101.

[†] Permanent affiliation: P. Kapitza Institute for Physical Problems, ul. Kosygina 2, 117334 Moscow, Russia.

- [1] Y. Mizuno *et al.*, Phys. Rev. B **57**, 5326 (1998).
- [2] M. Takano, J. Supercond. **7**, 49 (1994).
- [3] K. Ishida *et al.*, Phys. Rev. B **53**, 2827 (1996).
- [4] S. Gopalan *et al.*, Phys. Rev. B **49**, 8901 (1994); E. Dagotto, T. M. Rice, Science **271**, 618 (1996).
- [5] M. Matsuda, K. Katsumata, J. Magn. Magn. Mater. **140-145**, 1671 (1995).
- [6] F. D. M. Haldane, Phys. Rev. B **25**, 4925 (1982);
- [7] D. Allen and D. Sénéchal, Phys. Rev. B **55**, 299 (1997).
- [8] S. White, I. Affleck, Phys. Rev. B **54**, 9862 (1996).
- [9] R. Chitra *et al.*, Phys. Rev. B **52**, 6581 (1995).
- [10] Normand B. *et al.*, Phys. Rev. B **56**, R5736 (1997).
- [11] H. Bethe, Z. Phys. **71**, 205 (1931).
- [12] L. P. Regnault *et al.*, Phys. Rev. B, **53**, 5579, (1996).
- [13] Chr. L. Teske and Hk. Müller-Buschbaum, Z. Anorg. Allg. Chem. **371**, 325 (1969).
- [14] N. Motoyama *et al.*, Phys. Rev. Lett. **76**, 3212 (1996).
- [15] M. Tanaka *et al.*, PHYSICA C **261**, 309 (1996).
- [16] H. Ohta *et al.*, J. Phys. Soc. Jpn. **61**, 3370 (1992).